Vortices in Bose-Einstein condensates with dominant dipolar interactions

M. Abad, M. Guilleumas, R. Mayol, and M. Pi
Departament d'Estructura i Constituents de la Matèria, Facultat de Física, and IN2UB, Universitat de Barcelona, E–08028 Barcelona, Spain

D. M. Jezek
Departamento de Física, Facultad de Ciencias Exactas y Naturales, Universidad de Buenos Aires, RA-1428 Buenos Aires, Argentina and Consejo Nacional de Investigaciones Científicas y Técnicas, Argentina

(Dated: May 19, 2009)

We present full three-dimensional numerical calculations of single vortex states in rotating dipolar condensates. We consider a Bose-Einstein condensate of ^{52}Cr atoms with dipole-dipole and s-wave contact interactions confined in an axially symmetric harmonic trap. We obtain the vortex states by numerically solving the Gross-Pitaevskii equation in the rotating frame with no further approximations. We investigate the properties of a single vortex and calculate the critical angular velocity for different values of the s-wave scattering length. We show that, whereas the standard variational approach breaks down in the limit of pure dipolar interactions, exact solutions of the Gross-Pitaevskii equation can be obtained for values of the s-wave scattering length down to zero. The energy barrier for the nucleation of a vortex is calculated as a function of the vortex displacement from the rotation axis for different values of the angular velocity of the rotating trap.

PACS numbers: 03.75.Lm, 03.75.Hh, 03.75.Nt

I. INTRODUCTION

The experimental realization of a Bose-Einstein condensate of chromium atoms [1, 2] has encouraged research on the new field of dipolar gases at very low temperature. An ultracold gas of chromium atoms is a very suitable system for studying dipolar condensates because, in contrast to alkali atoms, ^{52}Cr atoms possess an anomalously large magnetic dipole moment. Moreover, the magnitude and sign of the s-wave scattering length between ^{52}Cr atoms, and therefore the strength of the contact interaction, can be experimentally controlled through Feshbach resonances [3, 4].

While the contact interaction is isotropic, the dipolar potential is anisotropic and long range. The atom-atom interaction is then determined by the balance of both potentials, giving rise to interesting phenomena in a dipolar Bose-Einstein condensate (BEC). One of them is their stability, which in contrast to s-wave condensates crucially depends on the trap geometry. In addition, there are other factors that affect the stability of the condensate, such as the scattering length, the magnetic (or electric) moment of the atoms and the number of trapped dipoles. The problem of stability and collapse in dipolar condensates has been the subject of intensive experimental [5–7] and theoretical investigations [8–12].

Another interesting feature is the appearance of new structured biconcave ground states for certain values of the strength of the dipolar interaction and the harmonic trap anisotropy [11, 12]. In contrast to condensates with the maximum of the density at the center, which have a roton-like excitation spectrum, these biconcave condensates become unstable due to angular excitations [12].

An important issue that is presently under investigation is the superfluid character of dipolar condensates. The presence of quantized vortices is a clear signature of superfluidity in quantum systems [13]. Dipolar condensates constitute a unique testing ground of the interplay between different interatomic interactions in the superfluid properties. Since the s-wave scattering length a can be experimentally controlled, it is appealing to study vortex states in different regimes, going from a pure dipolar (i.e. $a = 0$) to a pure contact interaction condensate, passing through BECs with both s-wave and dipolar interactions. As a tends to zero, the dipolar interaction becomes comparatively stronger and its effect on the nucleation of vortices is enhanced.

Vortices in dipolar condensates have been studied within the Gross-Pitaevskii framework [14–16]. It has been shown that the presence of vortex states affects the stability of a dipolar condensate [14, 15] and that the effect of dipolar interactions on the critical angular velocity depends on the geometry of the trap [16]. In Ref. [15] the authors have focused on attractive contact interactions in quasi-two-dimensional rotating dipolar condensates, whereas in Ref. [14] an axially symmetric non-rotating condensate has been studied. In Ref. [16] a variational approach has been used to describe a vortex state in the dipolar Thomas-Fermi (TF) limit.

The stability of vortices in dipolar condensates has been recently adressed. In Ref. [17], the authors have studied the stability and excitations of singly and doubly quantized vortices in dipolar BECs, while in Ref. [18] a phase transition has been predicted between straight and twisted vortex lines. Also, the transverse instability of vortex lines has been studied in Ref. [19].

In this work we consider vortex states in three-dimensional (3D) rotating dipolar condensates. Our aim

is to investigate the effect of the dipolar interaction on the vortex properties when the contact interaction is low enough to consider that the dipole-dipole interaction is dominant. To this end, we use a full 3D approach to numerically solve the Gross-Pitaevskii equation (GP). We concentrate on dipolar condensates with s-wave scattering length approaching zero and, in particular, we study the structure of the vortex core and obtain the critical rotation frequency necessary to nucleate a vortex. We also evaluate the energy barrier for vortex formation as a function of the vortex distance from the trap center.

This work is organized as follows. In Sec. II we describe the theoretical framework and the system under study. In Sec. III we revisit some properties of the ground state of dipolar BECs. In Sec. IV we investigate the formation of a centered vortex in a rotating frame, and in Sec. V we present the calculation of the nucleation barrier. Finally, a summary and concluding remarks are offered in Sec. VI.

II. THEORETICAL FRAMEWORK

We consider a Bose-Einstein condensate of N chromium atoms at zero temperature, confined by an axially symmetric harmonic potential

$$V_{\rm trap}(\mathbf{r}) = \frac{m}{2}\left(\omega_\perp^2 r_\perp^2 + \omega_z^2 z^2\right), \tag{1}$$

where $r_\perp^2 = x^2 + y^2$, m is the atomic mass, and $\omega_\perp$ and ω_z are the radial and axial angular trap frequencies, respectively. The aspect ratio of the trapping potential is $\lambda = \omega_z/\omega_\perp$. We shall only consider pancake shape condensates, in which case $\lambda > 1$ [20].

Since ^{52}Cr has a large magnetic dipole moment, $\mu = 6\mu_B$ (μ_B is the Bohr magneton), chromium atoms interact not only via s-wave contact interactions but also via the dipole-dipole interaction, which can be written as:

$$v_{\rm dip}(\mathbf{r}-\mathbf{r}') = \frac{\mu_0\mu^2}{4\pi}\frac{1-3\cos^2\theta}{|\mathbf{r}-\mathbf{r}'|^3}, \tag{2}$$

where μ_0 is the vacuum permeability, $\mathbf{r}-\mathbf{r}'$ is the distance between the dipoles, and θ is the angle between the vector $\mathbf{r}-\mathbf{r}'$ and the dipole axis, which we take to be z. In this configuration the dipoles are situated head to tail along the z axis. The dipolar interaction is then attractive along the magnetization direction and repulsive in the perpendicular one. Since we are considering a pancake geometry, this interaction is mainly repulsive.

In the mean-field framework, the GP equation provides a good description of a weakly interacting dipolar BEC, provided that the dipolar interaction is not too large. In order to investigate vortex states, we assume that the condensate is rotating around the symmetry axis z with angular frequency Ω. Using the imaginary-time propagation method in 3D we obtain the solutions of the GP equation in the rotating frame:

$$\left[-\frac{\hbar^2}{2m}\nabla^2 + V_{\rm trap} + g\,|\psi(\mathbf{r})|^2 + V_{\rm dip}(\mathbf{r}) - \Omega\hat{L}_z\right]\psi(\mathbf{r}) = \tilde{\mu}\,\psi(\mathbf{r}), \tag{3}$$

where $\psi(\mathbf{r})$ is the condensate wave function normalized to the total number of particles, $\hat{L}_z$ is the angular momentum operator along the z axis and $\tilde{\mu}$ is the chemical potential. The contact interaction potential is characterized by the coupling constant $g = 4\pi\hbar^2 a/m$ and the mean-field dipolar interaction $V_{\rm dip}(\mathbf{r})$ is given by:

$$V_{\rm dip}(\mathbf{r}) = \int d\mathbf{r}' v_{\rm dip}(\mathbf{r}-\mathbf{r}')|\psi(\mathbf{r}')|^2 . \tag{4}$$

When the dipolar BEC is at rest, the ground state is obtained from Eq. (3) by setting $\Omega = 0$.

The dipolar term in Eq. (3) transforms the usual GP equation in a more complicated integro-differential equation. However, the dipolar interaction integral (4) can be evaluated by using fast-Fourier transform (FFT) techniques [21] and the introduction of a cutoff at small distances [22]. We have used the FFTW package [23] to compute the discrete Fourier transforms.

The energy density functional in the rotating frame has the standard GP form but with a new term, $E_{\rm dip}$, which is the interaction energy due to the dipole-dipole potential:

$$\begin{aligned} E[\psi] \quad &= E_{\rm kin} + E_{\rm trap} + E_{\rm int} + E_{\rm dip} + E_L = \\ &= \int \frac{\hbar^2}{2m}|\nabla\psi|^2 d\mathbf{r} + \int V_{\rm trap}\,|\psi|^2 d\mathbf{r} + \int \frac{g}{2}\,|\psi|^4 d\mathbf{r} + \\ &+ \frac{1}{2}\int V_{\rm dip}\,|\psi|^2 d\mathbf{r} - \Omega\int \psi^*\hat{L}_z\psi\, d\mathbf{r}. \end{aligned} \tag{5}$$

From scaling considerations (see Appendix A), one can show that the virial theorem for a dipolar condensate reads:

$$2E_{\rm kin} - 2E_{\rm trap} + 3E_{\rm int} + 3E_{\rm dip} = 0 . \tag{6}$$

The fulfillment of this expression constitutes a good check of the accuracy of the numerical solution. In all the numerical calculations presented here we have checked that the condition (6) is well satisfied.

For purely dipolar condensates, it is useful to introduce a dimensionless parameter that measures the effective strength of the dipolar interaction [12]:

$$D = \frac{N\,\mu_0\,\mu^2\,m}{4\pi\,\hbar^2\,a_\perp}, \tag{7}$$

where $a_\perp = \sqrt{\hbar/(m\omega_\perp)}$ is the transverse harmonic oscillator length that characterizes the radial mean size of the noninteracting condensate. Increasing the value of D is equivalent to increase the number of atoms in the trap or their dipolar moment.

For dipolar condensates with also contact interactions, one can introduce another dimensionless quantity to characterize the relative strength of the dipolar and s-wave interactions [24]:

$$\epsilon_{dd} = \frac{\mu_0\mu^2 m}{12\pi\hbar^2 a}. \tag{8}$$

This parameter is defined in such a way that a homogeneous BEC with $\epsilon_{dd} > 1$ is unstable [25]. It has been shown [26] that in the Thomas-Fermi limit a dipolar BEC also becomes unstable when $\epsilon_{dd} > 1$. In this work we mainly study systems with $a \to 0$ that are far from the TF limit. This means that ϵ_{dd} does not need to be smaller than one for the BEC to be stable and indeed we still find stable solutions for $\epsilon_{dd} > 1$.

III. GROUND STATE

Before studying vortex states it is interesting to characterize the ground state wave function of the system, $\psi_0(\mathbf{r})$. It can be obtained from the minimization of the total energy (5), that is, by solving the GP equation (3) in the laboratory frame ($\Omega = 0$). As a starting point, we have checked that the results of our full 3D calculation are in agreement with the stability diagram of a pure dipolar condensate in a pancake trap previously calculated [12].

The main effect of the dipolar interaction on the ground state of the system is to deform the condensate as compared to the s-wave case. This effect is a direct consequence of the anisotropy of the dipolar potential and depends on the specific trap that is considered. For a spherical trap, the effect of the dipolar interaction is to squeeze the cloud along the repulsive direction while stretching it in the attractive direction. Although this might be somewhat counter-intuitive, it is easily explained taking into consideration the particular shape of the dipolar potential (see, for instance, Ref. [27]): since the dipolar potential shows a saddle configuration with two minima along the magnetization axis (attractive direction) it is less expensive for the system to accommodate more dipoles along this direction than along the repulsive one, thus the cloud size becomes larger in the former and smaller in the latter.

However, the deformation of the condensate is different for non-spherical traps. In Fig. 1 we show the density profiles in the perpendicular and parallel directions to the magnetization axis (x and z, respectively) for three different condensates: a pure dipolar BEC, a pure s-wave BEC ($a = 5\,a_B$) and one with the two types of interactions. All of them contain $N = 10^5$ bosons in a trap with frequencies $\omega_\perp = 8.4 \times 2\pi$ s^{-1} and $\omega_z = 92.5 \times 2\pi$ s^{-1}. The asymmetry parameter of such a configuration is $\lambda = 11$ and the dipolar parameters take the values $D = 50$ and $\epsilon_{dd} = 3.03$.

In order to quantitatively analyze the deformation of the condensate, we compute the root-mean-square radii in the radial and axial directions, namely $R_\perp$ and R_z. Figure 1 shows that the deformation is different to the spherical case: the gas is stretched in both directions of space, even though the cloud aspect ratio $\kappa = R_\perp/R_z$ increases ($\kappa = 8.28$ for the s-wave case, $\kappa = 9.06$ for the purely dipolar case and $\kappa = 9.65$ when both interactions are considered) [28]. The difference now is that the condensate is tightly trapped in the z direction so

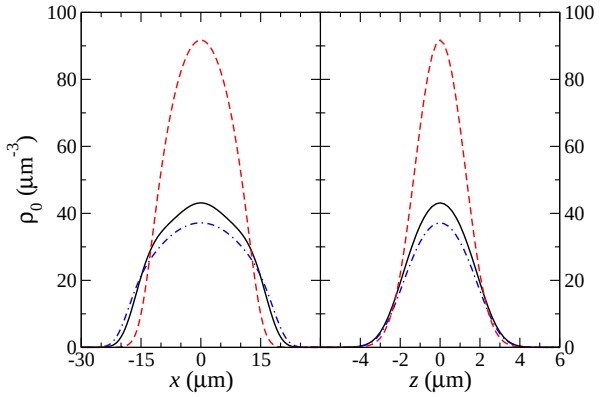

FIG. 1: (Color online) Ground state densities of pure s-wave (dashed line, with $a = 5\,a_B$), pure dipolar ($\mu = 6\mu_B$, solid line) and both s-wave and dipolar ($a = 5\,a_B$, $\mu = 6\mu_B$, dot-dashed line) condensates. They all correspond to the case $D = 50$, $\lambda = 11$, with $N = 10^5$ and $\omega_\perp = 8.4 \times 2\pi$ s^{-1}.

that the energy decrease achieved by putting more and more dipoles along the magnetization direction has to overcome a stronger trapping potential. The result of this energetic balance is that the system cannot accommodate so many atoms along the z axis, hence the cloud has to stretch in all directions.

On the other hand, the ground state of a dipolar condensate may present some stable density structures with the density maximum away from the center. They are usually found in isolated regions of the parameter space (D, λ) that are close to instability. This means that by increasing a little the value of D the condensate enters the unstable regime and overcomes a collapse which is thought to be of angular type [12]. Figure 2 shows the density profiles of two different stable ground state configurations of a pure dipolar ($a = 0$) condensate, one of them having a normal shape, while the other shows a biconcave structure. They both correspond to a condensate confined in a harmonic potential with asymmetry $\lambda = 11$ ($\omega_\perp = 8.4 \times 2\pi$ s^{-1} and $\omega_z = 92.5 \times 2\pi$ s^{-1}), but two different numbers of trapped atoms $N = 10^5$ (solid line) and 1.6×10^5 (dashed line), which correspond to dipolar interaction parameters $D = 50$ and 80, respectively.

It is important to note that although the parameter D is well suited to determine the regions where the density presents a biconcave shape, it fails to characterize all the physics underlying purely dipolar condensates. Clearly, we need at least three parameters to properly describe such systems since we have three degrees of freedom, namely N, $\omega_\perp$ and ω_z.

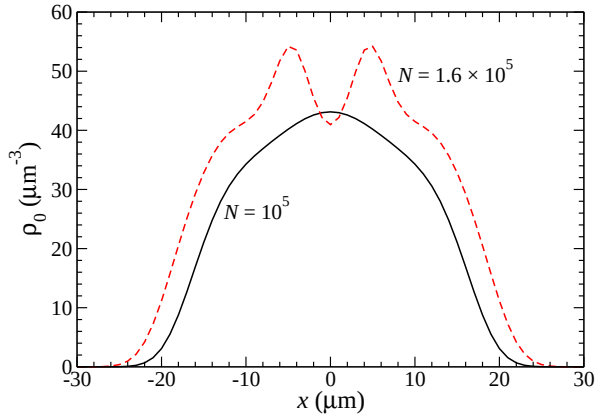

FIG. 2: (Color online) Density profile for the ground state configuration of pure dipolar BECs cointaining $N = 10^5$ (solid line) and $N = 1.6 \times 10^5$ (dashed line) atoms in the trap with $\omega_\perp = 8.4 \times 2\pi$ s^{-1} and $\omega_z = 92.5 \times 2\pi$ s^{-1}.

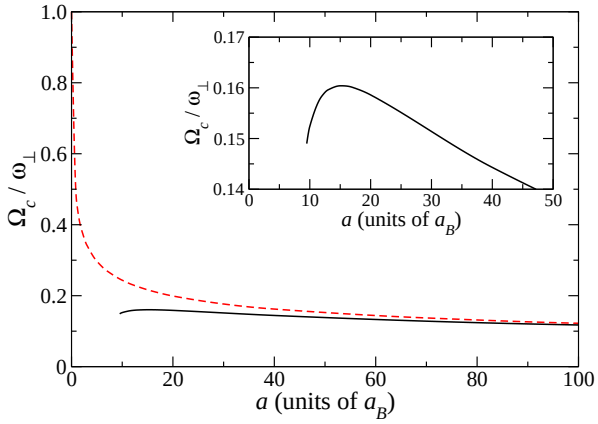

FIG. 3: (Color online) Critical angular velocity above which a singly quantized vortex is energetically favorable in a pancake trap with aspect ratio $\lambda = 5$, as a function of the s-wave scattering length. The solid line corresponds to s-wave plus dipolar interactions. The dashed line corresponds to only s-wave contact interaction. Inset: behavior of $\Omega_c(a)$ corresponding to both s-wave and dipolar interactions close to the instability limit.

IV. VORTEX STATES

A. Critical rotation frequency and vortex generation

The inclusion of vorticity is accompanied by an energy cost due to the appearance of angular momentum. Thus, in order to generate vortices the condensate must rotate. In a frame rotating at an angular frequency Ω about the z axis, the energy of the condensate carrying angular momentum L_z becomes $(E - \Omega L_z)$, where E and L_z are evaluated in the laboratory frame. At low rotation frequencies this energy is minimal without the vortex (ground state configuration). But if Ω is large enough the creation of a vortex can become favorable due to the $-\Omega \hat{L_z}$ term. This happens at the critical frequency Ω_c. The thermodynamical critical angular velocity for nucleating a singly quantized vortex is obtained by subtracting from the vortex state energy E_v in the laboratory frame the ground-state energy E_0, i.e., $\Omega_c = (E_v - E_0)/N\hbar$, and it provides a lower bound to the experimental critical angular velocity [29, 30].

Depending on the value of Ω, condensates with different number of vortices can be obtained, from a single vortex configuration at low angular velocities ($\Omega \sim \Omega_c$) to vortex lattices at high rotation frequencies. When the rotation frequency is close to the radial frequency of the trap the number of vortices becomes so large that the distance between them is smaller than the vortex cores, entering the strongly interacting regime [31]. In this work we are interested in single vortex configurations that are favorable when the angular velocity slightly exceeds the critical value.

We have numerically computed a vortex state by imprinting a phase to the initial wave function and solving the GP equation (3) in the rotating frame without fixing the vorticity during the minimization process. We have used the following ansatz for the initial wave function [32]:

$$\psi(\mathbf{r}) = \psi_0(\mathbf{r}) \, \frac{x + iy}{\sqrt{x^2 + y^2}} \,, \tag{9}$$

where ψ_0 is the ground state wave function. From this ansatz, it is straightforward to see that ψ and ψ_0 have the same density profile, but ψ has an imprinted velocity field which is irrotational everywhere except at the vorticity line (z axis). Moreover, ψ is an eigenstate of $\hat{L_z}$ with eigenvalue $N\hbar$.

Solving the GP equation (3), we have obtained, as expected, that for small values of Ω the system converges to a vortex-free configuration that corresponds to the ground state. However, for values of the angular frequency equal or slightly larger than the critical one, a centered vortex state configuration minimizes the energy. We have checked that the circulation is quantized around the vorticity line.

The value of the critical angular frequency Ω_c above which a vortex state is energetically favorable depends on the interaction parameters (scattering length, dipole moment), as well as on the number of atoms and on the trap geometry. We plot in Fig. 3 the critical angular velocity for vortex nucleation as a function of the scattering length, for a condensate with $N = 1.5 \times 10^5$, $\omega_\perp = 2\pi \times 200$ s^{-1}, $\lambda = 5$ and $D = 365.68$. These are the same parameters as in Ref. [16], where a variational ansatz was used to describe the vortex solution. By directly solving the dipolar GP equation without any further approximation we can go below the limit $a = 17.5\, a_B$ imposed by their variational ansatz and reach smaller scattering lengths. However, for $a < 9.5\, a_B$ the s-wave repulsion in the z direction is not strong enough to balance the attraction brought about by the dipole-dipole

interaction and the system becomes unstable.

As a reference we have also calculated the critical angular velocity necessary to nucleate a vortex in a non-dipolar condensate (with only s-wave interaction), see dashed curve in Fig. 3. In the noninteracting limit ($a = 0$) a vortex state corresponds to the first excited state with energy $E_v = E_0 + N\hbar\omega_\perp$, and therefore the critical angular frequency is $\Omega_c = \omega_\perp$ [30]. The inclusion of the dipolar interaction (solid curve) causes a decrease of the critical angular frequency, which becomes more sizeable for small s-wave interactions. As has been already pointed out [16], it follows from Fig. 3 that in a pancake trap it is easier to nucleate a vortex in the presence of dipolar interactions. This can be understood as follows: in a pancake shaped condensate, the interaction between dipoles aligned along the z axis is repulsive on average, hence the maximum density diminishes with respect to the pure s-wave value (see the variation of the central density in Fig. 1) and it becomes easier to take the atoms away from the z axis to nucleate a centered vortex. Thus, the effect of dipolar interactions is to decrease the critical angular frequency of vortex nucleation in a pancake shaped condensate.

We have found a good agreement between our results and those in Ref. [16] for large values of the scattering length, while for small values our $\Omega_c(a)$ curve exhibits a maximum around $a = 15a_B$ (see the inset in Fig. 3). The maximum value of the critical angular frequency is about $\Omega_c^{max} \simeq 0.16\,\omega_\perp$ at $a = 15a_B$, and corresponds to a dipolar condensate with $\epsilon_{dd} = 1.01$ and $D = 365.68$. Decreasing further the scattering length the critical angular velocity necessary to nucleate a vortex also decreases, in contrast to the general trend at large s-wave values.

The presence of a maximum value in the $\Omega_c(a)$ curve is a consequence of the balance between contact and dipolar interactions. To explore the origin of Ω_c^{max} we have also studied the critical angular velocity as a function of the s-wave scattering length for a system that remains stable at vanishing values of the scattering length, which corresponds to a pure dipolar condensate. We plot Ω_c in Fig. 4 for $D = 50$, $\omega_\perp = 2\pi \times 8.4$ s^{-1}, $\lambda = 11$, and $N = 10^5$. A detail of the behavior of $\Omega_c(a)$ corresponding to contact plus dipolar interactions for small values of the s-wave scattering length is shown in the inset. A maximum value of Ω_c appears also in Fig.4 around a scattering length $a \simeq 2a_B$, which corresponds to a dimensionless parameter $\epsilon_{dd} = 7.57$. In this case, the effect of the dipolar interaction becomes more clear: for a fixed value of the s-wave scattering length, the inclusion of the dipole-dipole interaction decreases the value of the critical angular velocity for vortex formation. In the limit of $a = 0$, that is for a pure dipolar condensate, Ω_c is around a factor 0.25 smaller than the non-interacting value.

The critical angular velocity for producing a vortex is plotted in Fig. 5 as a function of the number of atoms confined in the same trap as in Fig. 4, for a pure dipolar condensate (solid line) and for a condensate with only contact interaction with $a = 5a_B$ (dashed line). For

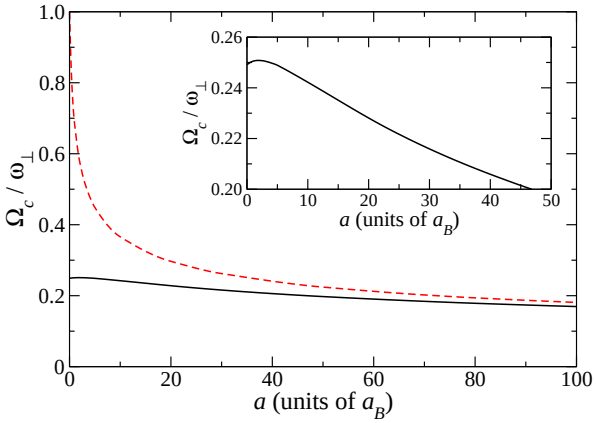

FIG. 4: (Color online) Critical angular velocity for a singly quantized vortex in a pancake trap with aspect ratio $\lambda = 11$, as a function of the s-wave scattering length. The solid line corresponds to s-wave plus dipolar interactions. The dashed line corresponds to only s-wave contact interaction. Inset: behavior of $\Omega_c(a)$ around $a \sim 0$ for a condensate with s-wave plus dipolar interactions.

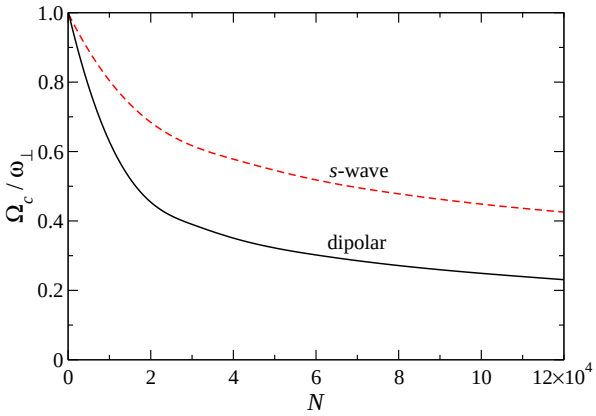

FIG. 5: (Color online) Critical angular velocity as a function of the number of atoms trapped in the same trap as in Fig. 4. The solid line corresponds to a pure dipolar condensate, and the dashed line to a condensate with only contact interaction ($a = 5a_0$).

a given number of atoms the effective repulsion of the dipolar interaction in a pancake shaped condensate is larger than the repulsive contact interaction; therefore, Ω_c is smaller in a pure dipolar condensate. However, both curves have a similar behavior: Ω_c decreases with increasing N, as the repulsion also increases.

B. Vortex core size

The vortex states we have obtained as a result of the 3D minimization process are straight vortex lines. For a condensate with only contact interaction a characteristic length for describing the core size of a vortex is given by the local healing length. In particular, the balance be-

tween the kinetic energy and the interaction energy fixes a typical distance over which the condensate wave function can heal. For a dilute Bose gas the healing length is given by $\xi = 1/\sqrt{8\pi n_0 a}$ [33], where the ground state density n_0 is evaluated at the vortex position. However, in the presence of dipole-dipole interactions this parameter does no longer provide a good estimate of the vortex core size.

A possible characterization has been given by O'Dell and Eberlein [16] assuming a variational ansatz for the vortex density profile:

$$\rho_v(r_\perp, z) = n_0 \left(1 - \frac{r_\perp^2}{R^2} - \frac{z^2}{Z^2}\right)\left(1 - \frac{\beta^2}{r_\perp^2 + \beta^2}\right), \quad (10)$$

where β, R and Z are variational parameters that describe the size of the core, and the radii in the transversal and axial direction, respectively. We want to note that for a pure s-wave condensate in the Thomas-Fermi approximation the product of the first two factors in Eq. (10) correctly describes the ground state density, identifying R and Z with the Thomas-Fermi radii. On the other hand, the third factor in the above formula satisfactorily models the vortex core shape. Clearly, the quotient between the vortex and ground state densities in the TF limit is zero at the vortex position and unity outside the vortex core. In particular, it is easy to verify that β corresponds to the radius at which this quotient is equal to $1/2$ at the $z = 0$ plane.

From the calculated vortex and ground state densities $\rho_v(\mathbf{r})$ and $\rho_0(\mathbf{r})$, we propose as a definition of the core radius β the $r_\perp$ value in the $z = 0$ plane that satisfies:

$$f(r_\perp = \beta, z = 0) = \frac{\rho_v(r_\perp = \beta, z = 0)}{\rho_0(r_\perp = \beta, z = 0)} = \frac{1}{2}. \quad (11)$$

This generalizes the definition given in Ref. [16]. We show in Fig. 6 the density profile as a function of x at $y = z = 0$, $\rho_v(x, y = 0, z = 0)$, corresponding to a vortex state of a condensate with dipolar plus contact interactions (solid line) and with only contact interaction (dashed line). Here $a = 5a_B$ and the parameters are the same as in Fig. 1: $N = 10^5$, $\lambda = 11$ and $\omega_\perp = 8.4 \times 2\pi$ s^{-1}, which correspond to $D = 50$. In the inset, the ratio f is depicted as a function of the distance to the vortex core for both cases. We can see that f does not take the value $f = 1$ outside the core. This is due to the fact that we are not in the TF regime and the structure of the BEC surface becomes important. When no dipolar effects are considered the deviation from the value $f = 1$ is larger. Nevertheless, Eq. (11) still provides a good definition of the vortex core.

Figure 7 shows the ratio $(\beta/R_\perp)$ of the vortex core size to the radial size of the disk-shaped condensate of Fig. 6 for different values of the s-wave scattering length. The effect of the dipolar interactions for large scattering lengths is to slightly increase the relative value of the core size with respect to the radial size of the condensate above the value of the pure s-wave case, as already discussed [16]. However, when $a < 20a_B$, the ratio $\beta/R_\perp$ is

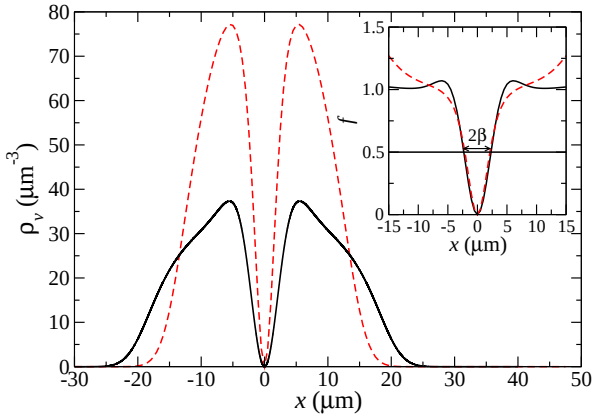

FIG. 6: (Color online) Vortex density profile as a function of x at $y = z = 0$ for BECs with contact ($a = 5a_B$) plus dipolar interaction (solid line) and only contact interaction (dashed line). The parameters are the same as in Fig. 1. Inset: f as a function of the distance to the vortex core for both cases; the value of the core radius β is also indicated.

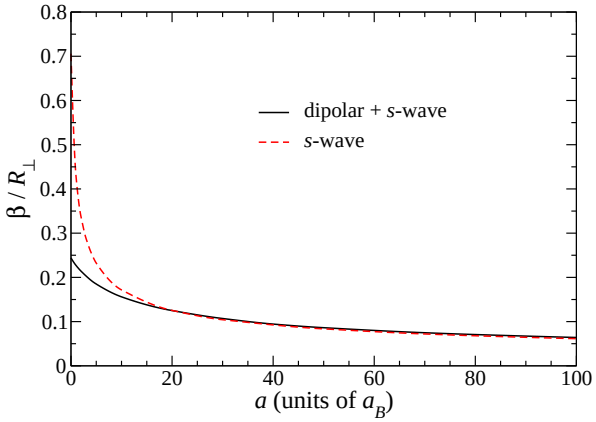

FIG. 7: (Color online) Ratio of the vortex core size (β) and the radial size of the condensate with respect to the scattering length for a disk-shaped condensate with $\lambda = 11$, $N = 10^5$ and $D = 50$. Solid curve: s-wave plus dipolar interactions. Dashed curve: only s-wave interactions.

larger for a condensate with dipolar interactions than in a pure contact interaction BEC. This is due to the small repulsive interaction brought by the dipole-dipole potential, which becomes noticeable only for small scattering lengths. This interaction has the effect of decreasing the central density of the condensate as compared to the pure s-wave case and this causes a smaller core radius and a broader ground state.

V. ENERGY BARRIER

The nucleation of a vortex is associated with the existence of an energy barrier in the configuration space between the initial vortex-free state and the final vortex state. Therefore, the system has to overcome this barrier

in order to nucleate a stable vortex. It is usually found that the vortex is nucleated at the boundary by surface excitations and it is stable at the center of the trap for rotational frequencies $\Omega \geq \Omega_c$. Then, the formation energy of a vortex can be obtained by calculating the energy of a single off-center vortex as a function of the vortex core position.

We have generalized the ansatz of an axially symmetric vortex line Eq. (9) to describe an off-center vortex at $\mathbf{r}_v = (x_v, y_v, z)$ [32, 34]:

$$\psi(\mathbf{r}) = \psi_0(\mathbf{r}) \, \frac{(x - x_v) + i\,(y - y_v)}{\sqrt{(x - x_v)^2 + (y - y_v)^2}} \, . \qquad (12)$$

Here the phase has been written in cartesian coordinates and corresponds to the azimuthal angle around the shifted position of the vortex core $\mathbf{r}_v$.

To calculate the energy of an off-center vortex line at a fixed distance $d = \sqrt{x_v^2 + y_v^2}$ from the z axis, $E(d, \Omega)$, we have solved the GP equation in the rotating frame taking Eq. (12) as initial wave function. In order to obtain the solution for the displaced vortex, which is not a minimum of Eq. (3), we have imposed that during the minimization process the initial nodal planes are kept constant, that is:

$$\mathrm{Re}\,[\Psi(x_v, y, z)] = 0 \quad \forall\, y, z \qquad (13)$$
$$\mathrm{Im}\,[\Psi(x, y_v, z)] = 0 \quad \forall\, x, z \; . \qquad (14)$$

With this method, the quantization of the circulation is assured in all cases, but the solutions are restricted to the case of straight vortex lines. An upper bound to the formation energy of the vortex is then obtained from the difference $\Delta E(d, \Omega) = E(d, \Omega) - E_0$.

We plot in Fig. 8 the vortex formation energy as a function of the vortex displacement from the center, corresponding to the same condensate as in Fig. 6 rotating at the critical rotational frequency Ω_c. The distance of the vortex core to the symmetry axis is expressed in units of $R_\perp$ of the corresponding ground state.

The dashed line corresponds to the pure contact interaction BEC (with $a = 5\,a_B$), the dash-dotted line to a condensate with contact plus dipolar interactions, and the solid line corresponds to a pure dipolar BEC ($D = 50$). Each curve has been calculated at the corresponding critical angular velocity (see Table I). It is interesting to note that even though $R_\perp$ is different for each curve, the three critical barriers have the same qualitative behavior as a function of the dimensionless displacement of the vortex core $d/R_\perp$. At Ω_c the centered vortex state and the vortex-free state have the same energy but they are separated by an energy barrier. The maximum of the barrier height ΔE is located around $d_{max}/R_\perp \sim 1.1$ for the contact interaction BEC and around $d_{max}/R_\perp \sim 1.2$ for the other cases. Since the radius of the condensate is larger for a system with dipolar plus contact interactions this means that, for the vortex state configuration at the barrier maximum, the distance between the vortex core and the z axis is larger than in the case of a pure dipolar

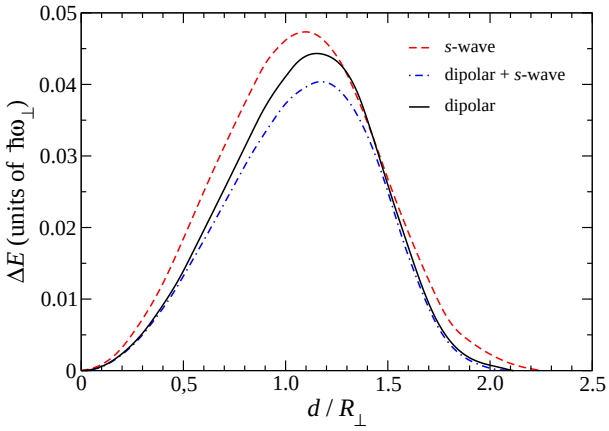

FIG. 8: (Color online) Energy barrier for the nucleation of a vortex in the rotating frame at $\Omega = \Omega_c$ as a function of the vortex displacement from the center. The dashed line corresponds to the pure contact interaction BEC (with $a = 5a_B$), the solid line corresponds to a pure dipolar BEC, and the dash-dotted line to a condensate with contact plus dipolar interactions.

condensate, which turns out to be also larger than the distance in a pure contact interaction BEC (see Table I).

For the sake of comparison we also give in Table I the barrier parameters at the critical frequency calculated in the TF approximation for a pure s-wave BEC. The barrier height and the position of the maximum can be obtained, respectively, from the expressions [35]

$$\Delta E(d_{max}, \Omega) = \frac{2}{5}\Omega_c \left(\frac{3}{5}\frac{\Omega_c}{\Omega}\right)^{3/2} \qquad (15)$$

and

$$d_{max} = \sqrt{3} R_\perp \sqrt{1 - \frac{3}{5}\frac{\Omega_c}{\Omega}} \; , \qquad (16)$$

where we have used that the TF radius in the radial direction and the corresponding root-mean-square value are related by $R_{TF} = \sqrt{3} R_\perp$. The critical frequency can be evaluated using [33]

$$\Omega_c = \frac{5\hbar}{6mR_\perp^2} \ln\left(\frac{0.671\sqrt{3}R_\perp}{\xi}\right) \; . \qquad (17)$$

Although the case we have considered does not really correspond to the TF limit ($Na/a_{ho} \approx 8$), we can see in Table I that this approximation can be used to obtain an estimate of the energy barrier, especially the location of its maximum, which matches very well the numerical result.

We plot in Fig. 9 the same curves as in Fig. 8 but calculated at larger angular velocities $\Omega > \Omega_c$, namely $\Omega = 0.48\ \omega_\perp$ for the pure contact interaction BEC with $a = 5\,a_B$ (dashed line) and $\Omega = 0.28\,\omega_\perp$ for both the pure dipolar BEC (solid line) and the condensate with the two

TABLE I: Characteristics of the energy barriers shown in Fig. 8.

Interaction	$R_\perp(\mu m)$	$\Omega_c(\omega_\perp)$	$d_{max}(\mu m)$	$d_{max}/R_\perp$	$\Delta E(\hbar\omega_\perp)$
$a=0$ $\mu=6\mu_B$	11.62	0.25	13.48	1.16	0.044
$a=5a_B$ $\mu=6\mu_B$	12.44	0.25	14.55	1.17	0.040
$a=5a_B$ $\mu=0$	9.16	0.45	9.98	1.09	0.047
$a=5a_B$ (TF)	10.84	0.38	11.87	1.09	0.071

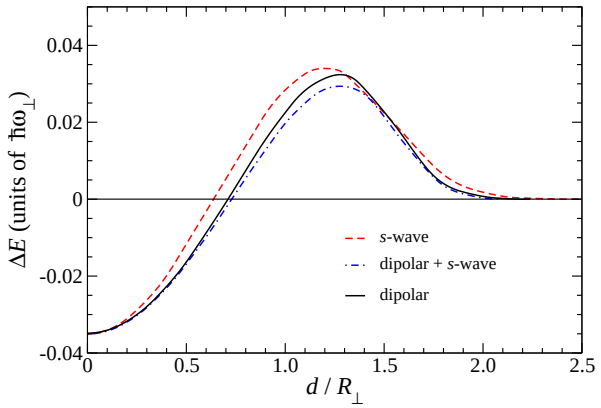

FIG. 9: (Color online) Vortex formation energy as a function of the vortex displacement from the center at angular velocities $\Omega > \Omega_c$. The dashed line corresponds to the pure contact interaction BEC (with $a = 5a_B$), the solid line corresponds to a pure dipolar BEC, and the dash-dotted line to a condensate with contact plus dipolar interactions.

types of interactions acting simultaneously (dash-dotted line).

As expected, for rotational frequencies larger than the corresponding critical one, the state with a centered vortex is preferable. However, the nucleation of the vortex is inhibited by the barrier separating the vortex-free state from the energetically favored vortex state which corresponds to the minimum energy configuration, at $d/R_\perp = 0$.

Finally, we have numerically checked that an off-center, unpinned vortex line located at distances larger than the position of the barrier maximum $d > d_{max}$ converges to the ground state. On the contrary, an off-center vortex located at $d < d_{max}$ converges to a centered vortex state.

VI. SUMMARY AND CONCLUDING REMARKS

In this paper we have adressed singly quantized vortex states in dipolar pancake shaped condensates. By fixing the dipole-dipole interaction and scanning the s-wave scattering length from $a = 100\,a_B$ to zero, we have been able to explore the vortex states in a dipolar condensate in three different regimes: when the two-body interaction is governed by the contact potential, when it is the dipole-dipole interaction that controls the properties of the gas and, finally, the region where both interactions are comparable.

We have reviewed some properties of the ground state of the dipolar condensate previously obtained in the bibliography. In particular, we have discussed its structure and have numerically solved the GP equation to obtain the new stable configurations which are not found in s-wave condensates. We have also discussed that the effect of the dipolar interaction on the effective size of the condensate depends strongly on the geometry of the confining potential. In a spherical trap, this anisotropic interaction tends to increase the size of the condensate in the direction perpendicular to the magnetization axis while reducing it in the parallel direction. However, we have found that in a pancake trap the radius is increased in both directions in such a way that the cloud aspect ratio also increases.

We have calculated the singly quantized vortex states of dipolar condensates in two different pancake configurations. We have obtained an excellent agreement with the results in Ref. [16] and have extended the study for scattering lengths as small as possible. We have seen that the effect of the dipolar interactions is to reduce the critical frequency for the nucleation of a vortex as compared to the s-wave case, and that a maximum in Ω_c appears at low scattering lengths (becoming more important near collapse). We have also obtained the structure of the vortex core and have shown that there exists a certain value of scattering length below which the dipolar effects become dominant.

Finally, we have characterized the energy barrier which has to be overcome to nucleate a vortex, both at the critical frequency and above it. To the best of our knowledge, this is the first study where energy barriers have been addressed in dipolar condensates. We have compared three different cases: a pure s-wave condensate, one with only dipolar interactions and a BEC with both types of interactions. Expressed as a function of the dimensionless vortex displacement, the barriers are of the same order but slightly different: for condensates with dipolar interactions, they are narrower and lower, indicating that it is energetically less expensive to nucleate a vortex in a dipolar BEC than in one with only contact interactions.

Acknowledgments

We thank Manuel Barranco for helpful discussions. This work has been performed under Grant No. PIP 5409 from CONICET and FIS2008-00421 from MEC (Spain). M. A. is supported by the Comission for Universities and Research of the Department of Innovation, Universities and Enterprises of the Catalan Government and the Eu-

ropean Social Fund.

Appendix A

In this appendix we obtain the virial theorem for a dipolar BEC from the density functional Eq. (5), by using the principle of scale invariance. The virial theorem results from the homogeneity properties of the kinetic and potential components of the energy of the many-body system with respect to a scaling transformation that preserves the normalization.

Considering the following transformation $\mathbf{r} \to \nu\mathbf{r}$, the condensate wave function scales as $\Psi(\mathbf{r}) \to \Psi_\nu(\mathbf{r}) = C\Psi(\nu\mathbf{r})$, where C is a normalization constant. The principle of scale invariance ensures that the norm of the wave function is preserved, that is

$$\int d\mathbf{r}\,|\Psi(\mathbf{r})|^2 = \int d\mathbf{r}\,|\Psi_\nu(\mathbf{r})|^2 = |C|^2 \int d\mathbf{r}\,|\Psi(\nu\mathbf{r})|^2 = N\ , \tag{A1}$$

which gives $C = \nu^{3/2}$. Using this result, it has already been shown (see, for instance, Ref. [36]) that the kinetic, harmonic potential and contact interaction terms in the energy functional (5) scale as

$$E_{\mathrm{kin},\nu} = \nu^2 E_{\mathrm{kin}}\ , \tag{A2}$$

$$E_{\mathrm{trap},\nu} = \frac{1}{\nu^2} E_{\mathrm{trap}}\ , \tag{A3}$$

$$E_{\mathrm{int},\nu} = \nu^3 E_{\mathrm{int}}\ . \tag{A4}$$

For the contribution of the dipolar energy to the functional, one can proceed in the same way and obtain its scaling law

$$\begin{aligned} E_{\mathrm{dip},\nu} &= \frac{1}{2}\frac{\mu_0\mu^2}{4\pi}\int d\mathbf{r}d\mathbf{r}'\,\frac{|\psi_\nu(\mathbf{r})|^2|\psi_\nu(\mathbf{r}')|^2}{|\mathbf{r}-\mathbf{r}'|^3}(1-3\cos^2\theta) \\ &= \frac{1}{2}\frac{\mu_0\mu^2}{4\pi}\int d\mathbf{r}d\mathbf{r}'\,\frac{\nu^6|\psi(\nu\mathbf{r})|^2|\psi(\nu\mathbf{r}')|^2}{|\mathbf{r}-\mathbf{r}'|^3}(1-3\cos^2\theta) \\ &= \frac{1}{2}\frac{\mu_0\mu^2}{4\pi}\nu^3\int d(\nu\mathbf{r})d(\nu\mathbf{r}')\,\frac{|\psi(\nu\mathbf{r})|^2|\psi(\nu\mathbf{r}')|^2}{|\nu\mathbf{r}-\nu\mathbf{r}'|^3}(1-3\cos^2\theta) \\ &= \nu^3 E_{\mathrm{dip}}\ . \end{aligned} \tag{A5}$$

Therefore the total energy of the system can be written as

$$E_\nu = \nu^2 E_{\mathrm{kin}} + \frac{1}{\nu^2}E_{\mathrm{trap}} + \nu^3 E_{\mathrm{int}} + \nu^3 E_{\mathrm{dip}}\ . \tag{A6}$$

Imposing the equilibrium condition

$$\left.\frac{dE_v}{d\nu}\right|_{\nu=1} = 0 \tag{A7}$$

one finds the virial theorem for a dipolar condensate, Eq. (6). Note that the rotating energy term E_L in Eq. (5) does not depend on the scaling parameter, and thus it does not contribute to the virial expression.

[1] A. Griesmaier, J. Werner, S. Hensler, J. Stuhler, and T. Pfau, Phys. Rev. Lett. **94**, 160401 (2005).

[2] Q. Beaufils, R. Chicireanu, T. Zanon, B. Laburthe-Tolra, E. Maréchal, L. Vernac, J.-C. Keller, and O. Gorceix, Phys. Rev. A **77**, 061601(R) (2008).

[3] J. Werner, A. Griesmaier, S. Hensler, J. Stuhler, T. Pfau, A. Simoni, and E. Tiesinga, Phys. Rev. Lett. **94**, 183201 (2005).

[4] T. Lahaye, T. Koch, B. Fröhlich, M. Fattori, J. Metz, A. Griesmaier, S. Giovanazzi, and T. Pfau, Nature **448**, 672 (2007).

[5] T. Koch, T. Lahaye, J. Metz, B. Fröhlich, A. Griesmaier, and T. Pfau, Nat. Phys. **4**, 218 (2008).

[6] J. Metz, T. Lahaye, B. Fröhlich, A. Griesmaier, T. Pfau, H. Saito, Y. Kawaguchi and M. Ueda, e-print arXiv:0901.1300v1 (2009).

[7] T. Lahaye, J. Metz, B. Fröhlich, T. Koch, M. Meister, A. Griesmaier, T. Pfau, H. Saito, Y. Kawaguchi, and M. Ueda, Phys. Rev. Lett. **101**, 080401 (2008).

[8] L. Santos, G. V. Shlyapnikov, P. Zoller, and M. Lewenstein, Phys. Rev. Lett. **85**, 1791 (2000).

[9] D. H. J. O'Dell, S. Giovanazzi, and C. Eberlein, Phys. Rev. Lett. **92**, 250401 (2004).

[10] N. G. Parker, C.Ticknor, A. M. Martin, and D. H. J. O'Dell, Phys. Rev. A **79**, 013617 (2009).

[11] O. Dutta and P. Meystre, Phys. Rev. A **75**, 053604 (2007).

[12] S. Ronen, D. C. E. Bortolotti and J. L. Bohn, Phys. Rev. Lett. **98**, 030406 (2007).

[13] R. J. Donnelly, *Quantized Vortices in Helium II* (Cambridge University Press, Cambridge, 1991).

[14] R. M. Wilson, S. Ronen, J. L. Bohn, and H. Pu, Phys. Rev. Lett. **100**, 245302 (2008).

[15] S. Yi and H. Pu, Phys. Rev. A **73**, 061602(R) (2006).

[16] D. H. J. O'Dell and C. Eberlein, Phys. Rev. A **75**, 013604 (2007).

[17] R. M. Wilson, S. Ronen, and J. L. Bohn, Phys. Rev. A **79**, 013621 (2009).

[18] M. Klawunn and L. Santos, eprint arXiv:0902.3058v1 (2009).

[19] M. Klawunn, R. Nath, P. Pedri and L. Santos, Phys. Rev. Lett. **100**, 240403 (2008).

[20] Even though 3D effects on vortex states should be more evident in cigar shaped configurations than in pancake ones, the stability of the condensate with $a \to 0$ is far more assured in the latter. Therefore, in order to reach stable configurations in the limit $a = 0$ we restrict ourselves to pancake geometries.

[21] K. Góral and L. Santos, Phys. Rev. A **66**, 023613 (2002).

[22] K. Góral, K. Rzażewski and T. Pfau, Phys. Rev. A **61**, 051601(R) (2000).

[23] M. Frigo and S. G. Johnson, Proc. IEEE **93**, 216 (2005).

[24] J.-P. Martikainen, M. Mackie, and K.-A. Suominen, Phys. Rev. A **64**, 037601 (2001).
[25] C. Menotti, M. Lewenstein, T. Lahaye, and T. Pfau, AIP Conference Proceedings **970**, 332 (2007).
[26] C. Eberlein, S. Giovanazzi, and D. H. J. O'Dell, Phys. Rev. A **71**, 033618 (2005).
[27] J. Stuhler, A. Griesmaier, T. Koch, M. Fattori, T. Pfau, S. Giovanazzi, P. Pedri, and L. Santos, Phys. Rev. Lett. **95**, 150406 (2005).
[28] If another definition for the radius is used (for instance, the FWHM) the actual values of $R_\perp$, R_z and κ are different but we checked that they predict the same behavior for the cloud aspect ratio.
[29] F. Dalfovo, S. Giorgini, L. P. Pitaevskii, and S. Stringari, Rev. Mod. Phys. **71**, 463 (1999).
[30] A. L. Fetter and A. A. Svidzinsky, J. Phys.: Condens. Matter **13**, R135 (2001).
[31] N. R. Cooper, E. H. Rezayi, and S. H. Simon, Phys. Rev. Lett. **95**, 200402 (2005); J. Zhang and H. Zhai, Phys. Rev. Lett. **95**, 200403 (2005); S. Komineas and N. R. Cooper, Phys. Rev. A **75**, 023623 (2007).
[32] D. M. Jezek, P. Capuzzi, and H. M. Cataldo, J. Phys. : At. Mol. Opt. Phys. **41**, 045304 (2008).
[33] E. Lundh, C. J. Pethick, and H. Smith, Phys. Rev. A **55**, 2126 (1997).
[34] A. L. Fetter, e-print arXiv:0801.2952
[35] M. Krämer, L. P. Pitaevskii, S. Stringari, and F. Zambelli, Laser Physics **12**, 113 (2002).
[36] D. M. Jezek, M. Barranco, M. Guilleumas, R. Mayol, and M. Pi, Phys. Rev. A **70**, 043630 (2004).